# Measurement of Longitudinal Emittance Growth Using a Laser-Induced Neutralization Method*

V. W. Yuan, R. Garcia, K. F. Johnson, K. Saadatmand,† O. R. Sander,
D. Sandoval, and M. Shinas
Los Alamos National Laboratory, Los Alamos, NM 87545

## Abstract

A laser-induced neutralization technique, LINDA, has been used to study the longitudinal emittance of the 5-MeV $H^-$ beam exiting the drift-tube Linac (DTL) of the Los Alamos Accelerator Test Stand (ATS). By using multiple laser intersection points, longitudinal emittance growths over drift distances of 23.6 and 30.6 cm were measured. Subsequently, a beam transport line, which consisted of one arm of a beam funnel, was substituted for the drift space. Measurements show that the elements of the funnel constrain emittance growth while the $H^-$ beam is contained within these transport elements.

## 1 Introduction

The Laser-Induced Neutral Diagnostic Approach (LINDA) [1] intersects an accelerator particle beam with short-duration (~23 ps) laser pulses which are used to measure the particle-beam longitudinal phase space. The rms longitudinal emittance at the point of laser intersection is quantitatively determined from the measurement. If two laser intersection points are employed simultaneously, the emittance growth in the beam-transport space between the intersection points can be determined. An experiment was performed on the 5-MeV $H^-$ beam of the ATS to measure the longitudinal emittance and its growth at the exit of the DTL section.

LINDA uses a short-duration laser pulse (see Figure 1) of small spatial width to intersect an $H^-$ beam bunch of the accelerator. The photons in the laser pulse photoneutralize a slice (in phase) of the intersected $H^-$ microbunch, producing $H^0$s. The remaining charged $H^-$s are steered out of the beam line by a dipole magnet while the neutral $H^0$s continue across a drift space to a detector farther down the beamline. The neutralized $H^0$s are produced nearly instantaneously, and if monoenergetic, their arrival at the detector would be a delta function in time. But, because the neutralized particles possess a finite energy spread and the detector has a finite resolution, the detector signal is spread out in time, and a quantitative determination of the energy spread can be determined from the time width of the detector signal. By varying the instant of the laser firing and thereby sampling different slices (in phase) of the beam bunch, the full longitudinal phase space of the beam can be reconstructed (see Figure 2a). A contour plot of this structure is shown in Figure 2b.

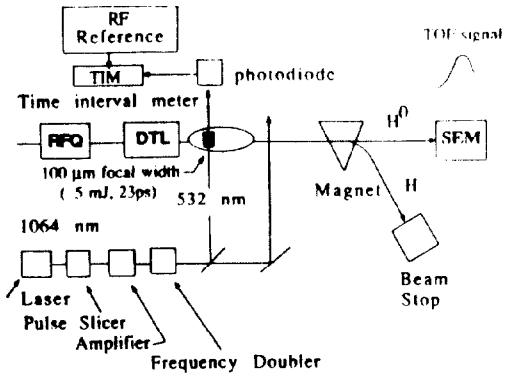


Figure 1: Schematic of LINDA experimental setup.

## 2 Experimental Setup

The experimental setup of Figure 1 contained a mode-locked Nd YAG laser with a fundamental frequency of 1.064 $\mu$m. The $H^-$ photoneutralization cross section [2] is a broad peak that does not vary by more than a factor of 2 over a wavelength range of 500 to 1400 nm. The output of the laser was pulse sliced, amplified, and frequency doubled, resulting in short-duration pulses at 532 nm. After frequency doubling, the flux of photons was reduced by 60% and the photodetachment cross section was ~17% smaller than with the 1064 nm fundamental, but the time duration of the laser pulses was shortened from 32 ps to 23 ps.

The repetition rate of the laser was 5 Hz, and a series of optical mirrors and beam splitters divided the laser beam

*Work supported and funded by the US Department of Defense, Army Strategic Defense Command, under the auspices of the US Department of Energy.

†Grumman Corporate Research Center.

0-7803-0135-8/91$01.00 ©IEEE

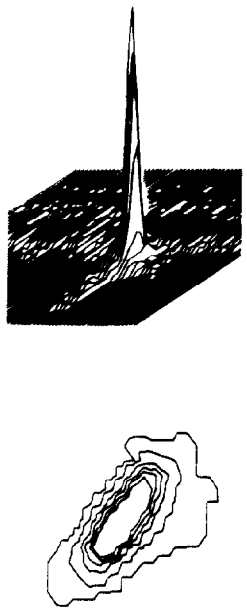

Figure 2: (a) Three-dimensional plot of longitudinal-emittance phase space at exit of ATS DTL. (b) Contour plot of the longitudinal phase space shown in figure 2A.

into separate paths that crossed the particle beam of the accelerator 6.3 cm and 29.9 cm past the end of the DTL. In a later run, the downstream crossing point was changed to a distance of 36.9 cm downstream of the DTL. In any laser firing, microbunches of the particle beam were intersected by the laser at one or the other of the crossing points, but not simultaneously at both.

The temporally short laser pulse neutralized a short phase slice of a beam micropulse. The neutralized beam particles were magnetically separated from the remaining charged particles in the beam, and their time-of-flight (TOF) arrival was recorded with a secondary-emission monitor (SEM). The SEM signal was digitized with a Tektronix AD7912 waveform digitizer, and the time of the laser firing within the micropulse was determined using a Nanofast 536-10B time-interval meter.

# 3 Phase Resolution

The laser pulse is characterized by its duration, $t_l$; its frequency, $f_l$; and the spatial width of its focus at the point of intersection, $w_l$. Each microbunch of the particle beam also occupies a certain spread in space, $w_b$, which is dependent on the rf phase occupied by the bunch. For adequate phase resolution in the LINDA measurement, both the laser focus width, $w_l$, and the distance travelled by the particle beam (with velocity $v$) during the period of laser illumination, $d = vt_l$, must be small compared to $w_b$. This condition is signified by writing the inequality:

$$t_l + \frac{w_l}{v} \ll t_b ,$$

where $t_b$ $(=w_b/v)$ is the time duration occupied by the microbunch, and for good resolution $\ll$ signifies a factor of 6 or greater.

# 4 Neutralization Fraction

The neutralization fraction for each laser pulse depends on the flux of photons intercepting the particle beam, the cross section for neutralization at the frequency of the laser light, and the average time a beam particle spends in the light of the laser beam. This latter quantity, the illumination time $t_i$, is dependent on the width of the laser focus, $w_l$, and the distance, $d$, travelled by the beam particle in the time period for which the laser pulse is on. If $w_l > d$, then the time most particles spend in the beam is $\sim t_l$. On the other hand if $d > w_l$, then most of the particles pass in and out of the laser beam before the pulse terminates, and their illumination time is $\sim w_l/v$. The neutralization fraction $N/N_0$ for beam particles illuminated for a period $t_i$ by the laser is calculated by evaluating

$$N/N_0 = e^{-\sigma F t_i} ,$$

where $\sigma$ is the photodetachment cross section and $F$ is the photon flux.

# 5 Emittance Determination

The data from a LINDA run consist of a set of TOF profiles, one profile for each laser fire. Associated with each profile is the Nanofast timing value demarking the phase of the beam micropulse when the laser fired. Profiles from laser firings with the same phase value are averaged to give TOF profiles related to the energy-spread distribution for each phase. Extracting the actual energy-spread distribution of the beam requires correcting each observed TOF profile for 1) background contributions and 2) the finite resolution of the detector.

The finite resolution of the detector was measured in separate calibration experiments during which the SEM was moved to a position just downstream of the laser intersection point. An effective rms width for the resolution profile was determined through numerical convolution of the calibration profile with Gaussian distributions of various widths. Each resulting convolved profile was fit to a Gaussian shape to determine its width, and the ensemble of resulting widths was fit to a distribution function:

$$\sigma^2_{\rm conv} = \sigma^2_s + \sigma^2_{\rm res}$$

to determine the effective width of the resolution profile, $\sigma_{\rm res}$. The width, $\sigma_{\rm conv}$, is that of the convolved profile

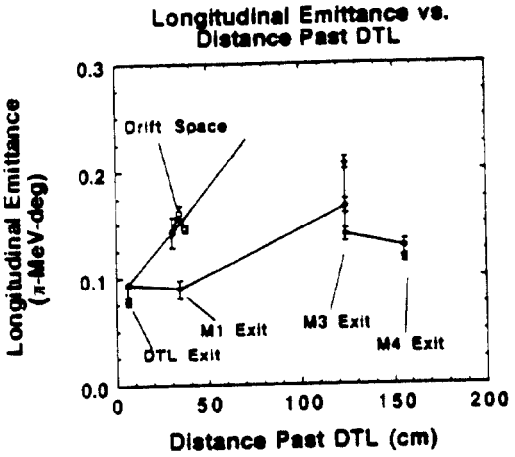


Figure 3: Measured (new results) longitudinal emittance growth in a drift space downstream of the ATS DTL. Continuous lines connect measurements made concurrently in time.

and $\sigma_s$ is the real signal width. In analyzing the data from each LINDA run, the averaged TOF profile (with background subtracted) for each phase bin was fit to a Gaussian shape to determine its width and amplitude. The observed width was then corrected using the previously determined effective detector resolution to give the actual signal width.

# 6 Results

Results from the emittance measurements taken at the exit of the DTL and at positions downstream following drift spaces of 23.6 cm and 30.6 cm are presented in Figure 3 and Table 1. They indicate an emittance of 0.73-0.93 $\pi$-MeV-deg as the beam leaves the DTL. Computer simulation studies using PARMTEQ were performed by the AT-1 group at Los Alamos [3], and the simulations predict an emittance 4 times larger than what is observed.

Emittance growths of 60% to 80% over drift distances of 23.6 cm and 30.6 cm are observed (see Figure 3). Previous measurements at Los Alamos observed emittance growths of 30% over a drift space of 11 cm, and computer-simulation studies duplicated the same magnitude of growth for the same distance of drift. The new data, however, indicate larger growths for the longer 24 to 31 cm drifts. So far, computer simulations of these longer drift distances have failed to produce a growth in emittance that exceeds 28% [4].

Subsequent to the emittance growth measurements, a beam transport line [5] that consisted of one arm of a beam funnel was substitued for the drift space. The transport line contained four permanent-magnet dipoles, fifteen permanent-magnet quadrupoles, four rf bunchers, and one rf deflector. The overall length of the transport line was 158 cm. Measured emittances at the exit of this single-arm

| Z (cm) | Longitudinal emittance ($\pi$· MeV · deg) |
|---|---|
| 6.3 | .0781 ± .0038 |
| 6.3 | .0934 ± .0015 |
| 29.9 | .1425 ± .0147 |
| 36.9 | .1462 ± .0031 |

Table 1: Longitudinal emittance values for points downstream of ATS Drift Tube Linac (DTL). Z is distance between laser intersection point and end of DTL.

funnel (M4 exit) are also shown in figure 3. The emittance growth after the funnel transport is no larger than that observed for a much shorter pure drift. We conclude that the funnel constrains emittance growth while the $H^-$ beam is contained within its transport elements.

# References

[1] W. B. Cottingame, G. P. Boicourt, J. H. Cortez, W. W. Higgins, O. R. Sander, and D. P. Sandoval, *Noninterceptive Techniques for the Measurement of Longitudinal Parameters for Intense $H^-$ Beams*, Proc. 1985 Particle Accelerator Conference, IEEE Trans. Nucl. Sci., Vol. 32, p. 1871, 1985.

[2] J. T. Broad and W. P. Reinhardt, "One- and two-electron photoejection from $H^-$: A multichannel J-matrix calculation," Phys. Rev. Vol. A14, p. 2159, Dec. 1976.

[3] F. Guy, Los Alamos National Laboratory, private communication.

[4] T. Bhatia, Los Alamos National Laboratory, private communication.

[5] K. F. Johnson, O. R. Sander, G. O. Bolme, J. D. Gilpatrick, F. W. Guy, J. H. Marquardt, K. Saadatmand, D. Sandoval, and V. Yuan, "A Beam Funneling Demonstration: Experiment and Simulation," in *Proceedings of the International Symposium on Heavy ion Inertial Fusion*, Monterey, CA, Dec. 1990.